

A “deformable section” model for the dynamics of suspension bridges. Part II: Nonlinear analysis and large amplitude oscillations

Vincenzo Sepe[†]

*Dipartimento di Progettazione, Riabilitazione e Controllo delle Strutture Architettoniche,
Università di Chieti, Pescara “G. D’Annunzio”, Viale Pindaro, 42, 65127 Pescara, Italy*

Mariella Diaferio[‡]

*Dipartimento di Ingegneria Civile e Ambientale (Sez. Strutture), Politecnico di Bari,
Via Orabona 4, 70125 Bari, Italy*

Giuliano Augusti^{‡‡}

*Dipartimento di Ingegneria Strutturale e Geotecnica, Università di Roma “La Sapienza”,
Via Eudossiana, 18, 00184 Roma, Italy*

(Received December 16, 2003, Accepted July 28, 2003)

Abstract. The classical two-degree-of-freedom (2-d-o-f) “sectional model” is of common use to study the dynamics of suspension bridges. It takes into account the first pair of vertical and torsional modes of the bridge and describes well global oscillations caused by wind actions on the deck, yielding very useful information on the overall behaviour and the aerodynamic and aeroelastic response; however, it does not consider relative oscillations between main cables and deck. On the contrary, the 4-d-o-f model described in the two Parts of this paper includes longitudinal deformability of the hangers (assumed linear elastic in tension and unable to react in compression) and thus allows to take into account not only global oscillations, but also relative oscillations between main cables and deck. In particular, when the hangers go slack, large nonlinear oscillations are possible; if the hangers remain taut, the oscillations remain small and essentially linear: the latter behaviour has been the specific object of Part I (Sepe and Augusti 2001), while the present Part II investigates the nonlinear behaviour (coexisting large and/or small amplitude oscillations) under harmonic actions on the cables and/or on the deck, such as might be generated by vortex shedding. Because of the discontinuities and strong nonlinearity of the governing equations, the response has been investigated numerically. The results obtained for sample values of mechanical and forcing parameters seems to confirm that relative oscillations cannot a priori be excluded for very long span bridges under wind-induced loads, and they can stimulate a discussion on the actual possibility of such phenomena.

Keywords: suspension bridges; wind effects; sectional model; nonlinear dynamics; vortex shedding.

[†] Associate Professor

[‡] Assistant Professor

^{‡‡} Professor

1. Introduction

The 4-d-o-f “*deformable section*” model proposed in this paper extends the 2-d-o-f rigid section model classically used to describe the response of long span suspension bridges under wind loading, and draws the attention on the possibility of relative displacements and rotations between the deck and the main cables, allowed by the deformability of the suspending hangers. These are assumed linear elastic in tension and ineffective in compression (Fig. 1): thus, the proposed model is able to describe the oscillations of the bridge for the whole range of behaviour of the hangers. To the writers’ knowledge, no analytical sectional model had before ever been related to these relative oscillations.

As long as the hangers remain taut, the oscillations are small and essentially linear but, outside this range, some or all the hangers of a row (pre-stressed by the dead loads in the reference configuration) may become slack and the generalised stiffness of the sectional model is greatly reduced (cf. Part I of this paper: Sepe and Augusti 2001). Because of the discontinuity and the consequent strong nonlinearity of the equations of motion in this range, the full behaviour of the proposed model can be found only by step-by-step integration.

In Part I some related previous works have been discussed; then, the conditions have been determined that guarantee small amplitude oscillations (hangers always taut) around the equilibrium configuration under dead loads: this analysis has shown that the possibility of the large amplitude oscillations (with alternatively hangers loosening and tightening) cannot be excluded for long span bridges subject to winds with speeds within realistic limits.

The present Part II investigates the nonlinear dynamic behaviour of the model for wind-induced forces both on the main cables and on the deck: several cases are treated numerically and the results discussed. In particular, it will be shown that the negative displacements between main cables and deck (hanger ends “getting closer”) can become one or two order of magnitude larger than the displacements due to the global oscillations described by the classical 2-d-o-f model, especially in case of small structural damping.

In order to make this part of the paper self-contained, in Section 2 the equations of motion are presented again and the main results of Part I recalled.

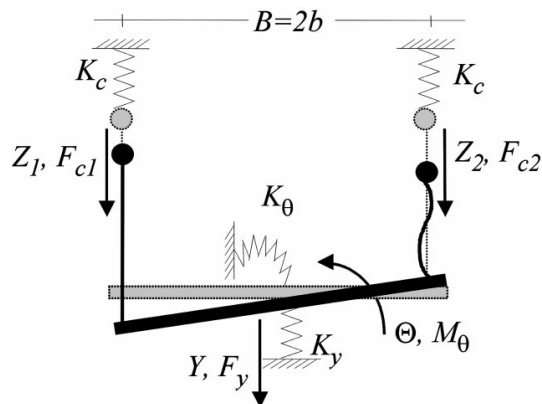


Fig. 1 The 4-d-o-f “deformable section” model

2. The model: equations of motion

In the proposed model, while cables and deck are assumed to behave elastically, hangers are considered as linear elastic in tension and ineffective in compression (Fig. 1). However, the hangers are pre-stressed in the reference configuration by the deck weight: therefore, the unilateral behaviour is significant only if the amplitude of the relative displacement ΔY_i between main cables and deck becomes larger than the elastic elongation ΔY_0 of the hangers in the reference configuration (Fig. 2). Note also that no other source of nonlinearity is introduced in the model: the restraints on the cables and the deck are assumed as linear, without considering any “geometrical nonlinearity”.

In order to obtain a still relatively simple model, it is assumed that the three principal components of the bridge, namely the main cables and the deck, oscillate with the same longitudinal shape $\psi(x)$, although not with the same amplitudes. As a consequence of this assumption, all sections behave in a similar way and therefore the bridge response can be described by a “sectional model”: in the present case, a “deformable section” model, that improves the classical 2-d-o-f rigid-section model, because it is able to account for relative vertical displacements between main cables and deck, made possible by the elasticity of the hangers in tension and their “slackness” in compression; the lateral displacements are neglected in both models.

Let $Y(t)$ and $\Theta(t)$ (Fig. 1) denote the generalised displacement and rotation of the deck related to the assumed pseudo-modal shape $\psi(x)$, while $Z_1(t)$ and $Z_2(t)$ denote the generalised displacement of the two main cables; let also m_c be the generalised mass of each cable and m_y, I the generalised mass and torsional inertia of the deck, respectively, while it is assumed that the mass of the hangers can be neglected with respect to m_c, m_y .

Indicating by the suffixes 1 and 2 each cable, the relevant equations of motion are (Sepe and Augusti 2001):

$$\begin{aligned}
 m_c \ddot{Z}_1 + 2\zeta_c \omega_c m_c \dot{Z}_1 + K_c Z_1 - \delta_1 K_{h0} (Y + b\Theta - Z_1) + (1 - \delta_1) K_{h0} \Delta Y_0 &= F_{c1}(t) \\
 m_c \ddot{Z}_2 + 2\zeta_c \omega_c m_c \dot{Z}_2 + K_c Z_2 - \delta_2 K_{h0} (Y - b\Theta - Z_2) + (1 - \delta_2) K_{h0} \Delta Y_0 &= F_{c2}(t) \\
 m_y \ddot{Y} + 2\zeta_y \omega_y m_y \dot{Y} + K_y Y + K_{h0} [\delta_1 (Y + b\Theta - Z_1) - (1 - \delta_1) \Delta Y_0 + \delta_2 (Y - b\Theta - Z_2) - (1 - \delta_2) \Delta Y_0] &= F_y(t) \\
 I \ddot{\Theta} + 2\zeta_\theta \omega_\theta I \dot{\Theta} + K_\theta \Theta + K_{h0} b [\delta_1 (Y + b\Theta - Z_1) - (1 - \delta_1) \Delta Y_0 - \delta_2 (Y - b\Theta - Z_2) + (1 - \delta_2) \Delta Y_0] &= M_\theta(t) \quad (1)
 \end{aligned}$$

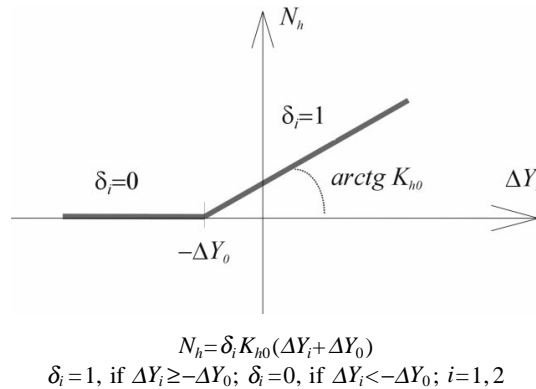


Fig. 2 Generalised force N_h transmitted by hangers between the main cables and the deck vs. the generalised relative displacement ΔY_i , according to Eq. (1) and Eq. (8)

where also damping terms ζ_c , ζ_y , ζ_θ have been introduced, while $b=B/2$ denotes the half-width of the deck (Fig. 1); ω_c , ω_y , ω_θ are the natural pulsations (angular frequencies) of cables and deck, K_c , K_y , K_θ , K_{h0} are respectively the vertical (geometrical) generalised stiffness of each cable, the vertical and torsional generalised stiffness of the deck and the generalised stiffness of a row of hangers, and δ_i ($i=1,2$; $0 \leq \delta_i \leq 1$) is a stiffness-reduction coefficient (in principle, time-dependent) that takes into account the possible “slacking” of the hangers (and depends on the amplitude of oscillations, being related to how many hangers go slack). Eqs. (1) include the forcing terms (vertical forces and moments) F_{c1} , F_{c2} , F_y , M_θ acting on the main cables and on the deck (as shown in Fig. 1), while no loads on the hangers have been considered.

Introducing non-dimensional variables and parameters

$$q_1 = \frac{Z_1}{b}, \quad q_2 = \frac{Z_2}{b}, \quad q_3 = \frac{Y}{b}, \quad q_4 = \Theta, \quad d_0 = \frac{\Delta Y_0}{b}$$

$$f_1 = \frac{F_{c1}}{m_c g}, \quad f_2 = \frac{F_{c2}}{m_c g}, \quad f_3 = \frac{F_y}{m_y g}, \quad f_4 = \frac{M_\theta b}{I g} \quad (2)$$

$$\beta_1 = \frac{m_c}{m_y}, \quad \beta_2 = \frac{m_c b^2}{I}, \quad \omega_h^2 = \frac{K_{h0}}{m_c}$$

where g is the gravitational acceleration, the equations of motion become

$$\begin{aligned} \ddot{q}_1 + 2\zeta_c \omega_c \dot{q}_1 + \omega_c^2 q_1 - \delta_1 \omega_h^2 (q_3 + q_4 - q_1) + (1 - \delta_1) \omega_h^2 d_0 &= \frac{g}{b} f_1(t) \\ \ddot{q}_2 + 2\zeta_c \omega_c \dot{q}_2 + \omega_c^2 q_2 - \delta_2 \omega_h^2 (q_3 - q_4 - q_2) + (1 - \delta_2) \omega_h^2 d_0 &= \frac{g}{b} f_2(t) \\ \ddot{q}_3 + 2\zeta_y \omega_y \dot{q}_3 + \omega_y^2 q_3 + \beta_1 \omega_h^2 [\delta_1 (q_3 + q_4 - q_1) - (1 - \delta_1) d_0 + \delta_2 (q_3 - q_4 - q_2) - (1 - \delta_2) d_0] &= \frac{g}{b} f_3(t) \\ \ddot{q}_4 + 2\zeta_\theta \omega_\theta \dot{q}_4 + \omega_\theta^2 q_4 + \beta_2 \omega_h^2 [\delta_1 (q_3 + q_4 - q_1) - (1 - \delta_1) d_0 - \delta_2 (q_3 - q_4 - q_2) + (1 - \delta_2) d_0] &= \frac{g}{b} f_4(t) \end{aligned} \quad (3)$$

In all examples presented in this paper, the forcing terms have been assumed to vary harmonically with time (in fact, they are intended to represent wind-induced loads due to Kármán vortex shedding). With regard to the actions on the main cables, the amplitude f_c and the pulsation Ω_c are assumed to be the same for both cables, with a phase lag $\Delta\varphi$, i.e.,

$$f_1(t) = f_c \sin \Omega_c t, \quad f_2(t) = f_c \sin (\Omega_c t + \Delta\varphi) \quad (4)$$

It has been shown in the Part I of this paper (Sepe and Augusti 2001) that the phase lag $\Delta\varphi$ could significantly affect the dynamic response; it has also been shown that one of the values $\Delta\varphi=0$ (in-phase forcing) or $\Delta\varphi=\pi$ (forcing in phase-opposition) maximises the length variation of the hangers, and therefore could amplify the slacking effect. As an example, the value of $\Delta\varphi=\pi/4$ has been considered in the numerical investigations, to show how rich the dynamical response can be; on the other hand, the determination of the “true” value of $\Delta\varphi$ for a given specific problem is outside the aim of the present paper.

As for the actions on the deck, the force amplitude is denoted by f_d , and the moment M_θ is introduced by means of an eccentricity e_d :

$$f_3(t) = f_d \sin \Omega_d t, \quad f_4(t) = e_d f_3(t) \tag{5}$$

3. Linear elastic oscillations

3.1. Free oscillations

Linear elastic oscillations are obtained putting $\delta_1 = \delta_2 = 1$ into Eqs. (3). Assuming the damping coefficients $\zeta_c, \zeta_y, \zeta_\theta$ to be zero, a classical eigenvalue analysis yields the four natural pulsations $\omega_1, \omega_2, \omega_3, \omega_4$ of the sectional model. As shown in Part I, the first two natural modes correspond to motions with small deformations of the hangers (denoted in the following as *global* vertical and torsional modes, Fig. 3(a),(b)) and their pulsations ω_1, ω_2 are much lower than the pulsations ω_3, ω_4 corresponding to *relative* modes (i.e., oscillations with cables and deck moving vertically out of phase, Fig. 3(c),(d)).

3.2. Forced oscillations: limit of linear behaviour

As anticipated at the beginning of Section 2, if ΔY_1 and ΔY_2 are the generalised relative displacements of the two rows of hangers, respectively, and ΔY_0 the corresponding elastic elongation of the hangers due to the weight of the deck, the response of the model is certainly elastic linear as long as

$$\Delta Y_1(t) \geq -\Delta Y_0 ; \quad \Delta Y_2(t) \geq -\Delta Y_0 \tag{6}$$

Therefore, the conditions

$$\max |\Delta Y_1(t)| = \Delta Y_0 ; \quad \max |\Delta Y_2(t)| = \Delta Y_0 \tag{7}$$

provide a sure boundary for the elastic behaviour of the model.

Lines corresponding to Eqs. (7) have been obtained in Part I assuming harmonic forces f_1, f_2 of the same amplitude f_c , and pulsation Ω_c acting only on the cables (cf. Eq. (4)) with a given phase-

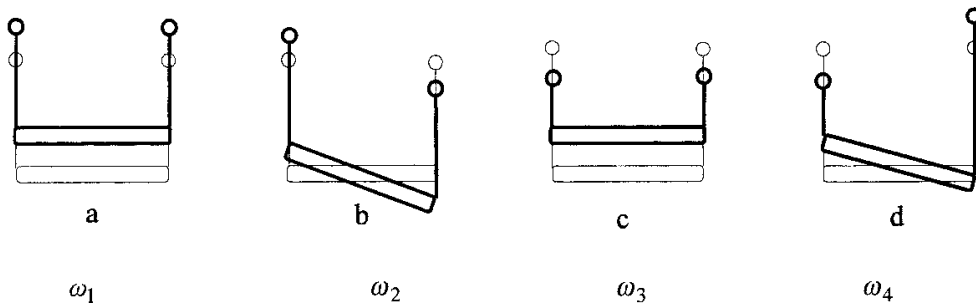


Fig. 3 Diagram of the linear modes of the 4-d-o-f sectional model and corresponding angular frequencies

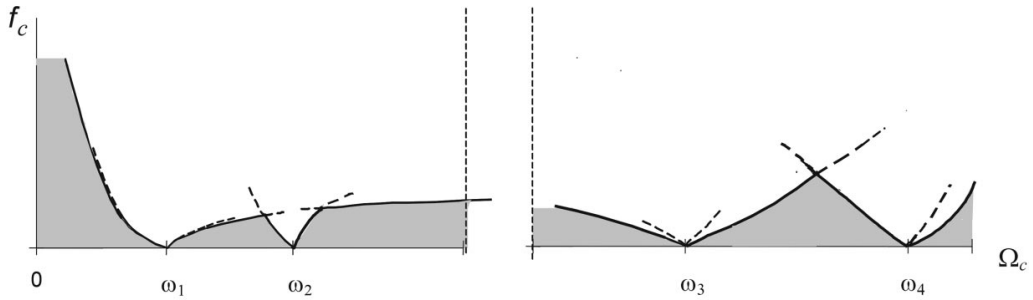


Fig. 4 Diagrammatic non-dimensional loading amplitude $f_c = F_c / m_c g$ of the vortex-shedding force on the main cables corresponding to upper limit of elastic behaviour (Eq. (3) for $\delta_i = 1$) vs. angular frequency Ω_c , for zero damping ($m_c g =$ cable weight). A numerical example is reported in Part I (Fig. 4, Tab. 1)

lag $\Delta\varphi$ ($f_3 = f_4 = 0$); this load condition enhances high frequency relative motions, complementary to slow global motions well described through the rigid section model and mainly due to actions on the deck.

Note that $\Delta\varphi = 0$ represents in-phase actions on the cables, that excite only vertical motions (global and relative), without torsional motions of the deck. In this case, in the high frequency range, the contribution of the global modes to the length variation of the hangers is negligible. Similarly, $\Delta\varphi = \pi$ represents actions in opposition of phase, and only the (global and relative) torsional modes develop.

For $\Delta\varphi$ different from 0 and π , both vertical and torsional modes are excited. However, it has been demonstrated (Part I) that the limit condition for arbitrary $\Delta\varphi$ is given by the lower f_c value corresponding to either $\Delta\varphi = 0$ or $\Delta\varphi = \pi$, that can therefore be taken as a safe boundary for elastic response.

In the case of zero damping, all limit curves go obviously to zero ($f_c = 0$) in conditions of resonance, i.e., for $\Omega_c = \omega_i$ (with $i = 1, 2, 3$ or 4); an example of such a boundary is qualitatively shown in Fig. 4 (analogous to Fig. 4 of Part I). For small damping, the boundary presents hollows (i.e., small f_c values) in the vicinity of resonance ($\Omega_c \approx \omega_i$).

In the next section, cases that violate the elastic boundary (that in Part I have been shown to be not unrealistic) will be investigated.

4. Nonlinear analysis

When inequalities (6) are violated, the stiffness-reduction coefficients δ_i in Eq. (3) assume values between 0 and 1, that vary in time as a consequence of the amplitude of oscillations. In the numerical analyses, the simplifying and limit assumption has been introduced that the values of δ_i can only be either 0 or 1, depending on sign and value of the generalised relative displacement ΔY_i ($i = 1, 2$) between main cables and deck with respect to the elastic elongation ΔY_0 of the hangers in the reference configuration, namely (Fig. 2),

$$\delta_i = 1, \text{ if } \Delta Y_i \geq -\Delta Y_0; \delta_i = 0, \text{ if } \Delta Y_i < -\Delta Y_0; i = 1, 2 \tag{8}$$

This assumption of discontinuity in the stiffness of the cable-to-deck connections, that would

seem trivial if the section model shown in Fig. 1 were considered in isolation, represents only a limit approximation when the section model is used to describe the dynamics of the whole bridge; in fact, while it is very close to the real behaviour if the assumed $\psi(x)$ is a no-node shape (e.g., half-length of a sine wave, as in Part I), for different pseudo-modal shapes Eqs. (8) is only an approximation of the actual softening behaviour of the structure due to the unilateral characteristics of the secondary suspension system.

The discontinuities that are thus introduced in the equations of motion (3) call for a great attention in the search of the numerical solutions, that are very sensitive to initial conditions; moreover, multiple stable and/or unstable solutions may coexist.

Inspection of Eqs. (2)-(3) shows that the ten parameters ω_c , ω_y , ω_θ , ω_h , ζ_c , ζ_y , ζ_θ , β_1 , β_2 , b fully define the mechanical properties of the system, on which the four natural pulsations of the bridge in the elastic range ω_1 , ω_2 , ω_3 , ω_4 depend.

Six parameters, namely ω_1 , ω_2 , ω_3 , β_1 , β_2 , b , have been varied in the performed investigation, while the other parameters, in accord with Part I and previous examples (Augusti, *et al.* 1997, Augusti and Sepe 1999), have been given the constant values

$$\omega_y=0.10 \text{ rad/s}, \zeta_c=0.002, \zeta_y=0.003, \zeta_\theta=0.005$$

except Figs. 9, 10, 11 where the damping coefficients have been assumed smaller to highlight some characteristics of internal resonance. Note that ω_y is the pulsation of the first bending mode of the deck alone, as it were isolated from the other parts of the structure. The values attributed to the parameters are shown in Table 1, where, instead of ω_1 , ω_2 , ω_3 , the ratios

$$\alpha_1 = \frac{\omega_1}{\omega_y} \quad \alpha_2 = \frac{\omega_2}{\omega_1} \quad \alpha_3 = \frac{\omega_3}{\omega_1} \quad (9)$$

are indicated. The ratio α_1 between the pulsation ω_1 of the first *global* bending mode of the system and the pulsation ω_y of the analogous mode of the deck alone, underlines the contribution of the suspension (main cables plus hangers) to the *global* system stiffness; α_2 is the ratio between the pulsation ω_2 of the *global* linear torsional oscillation and the corresponding bending pulsation ω_1 ; finally, α_3 is the ratio between the pulsation ω_3 of the *relative* vertical deck-cables motion and the system *global* bending pulsation ω_1 , and therefore is an indication of the stiffness of the hangers, assumed to remain in the linear range of behaviour.

Table 1 shows also the values of the ratio $\alpha_4=\omega_4/\omega_3$ which, although depending on the other parameters, gives a direct indication on the possible internal resonance between vertical and torsional relative mode (that occurs for $\alpha_4=2$ and implies a substantial difference in the dynamic response of the system).

Like in the examples considered in Part I, also in this paper the pseudo-modal shape $\psi(x)$ has been always assumed as a sinusoidal half-wave, that presents displacements of the same sign along the whole span (no-node shape).

With regard to the loading conditions, harmonic actions (intended to mimic vortex shedding from the suspension cables or from the deck) have been considered, with pulsation Ω_c or Ω_d close to a natural pulsation of the system, i.e., such that they can synchronise with the structure in a relatively large range of wind speed (*lock-in*): more specifically, forcing pulsations close to the natural pulsations, ω_3 or ω_4 , of the relative motions between cables and deck (Fig. 3) have been considered. In these conditions, in fact, significant relative displacements between the main cables and the deck

Table 1 Cases considered in the numerical investigation, in combination with several harmonic actions on the main cables or on the deck. For all cases, $\omega_y=0.10$ rad/s

Case	$\alpha_1=\omega_1/\omega_y$	$\alpha_2=\omega_2/\omega_1$	$\alpha_3=\omega_3/\omega_1$	α_4	β_1	β_2	b (m)	Ref. Fig.
1	6	3	5	2.32	0.40	2.25	15	7,8,12
2	6	2.51	5	2	0.40	2.25	15	9,10,11
3	2	3	5	2.32	0.40	2.25	15	12
4	20	3	5	2.32	0.40	2.25	15	5,6,12
5	4	2	4	2.15	0.25	3.15	17.75	13
6	4	2	5	2.19	0.25	3.15	17.75	13
7	4	2	10	2.22	0.25	3.15	17.75	13
8	4	2	50	2.25	0.25	3.15	17.75	13
9	4	2	160	2.42	2.25	3.15	17.75	
10	4	3.23	10	2.32	0.25	3.15	17.75	
11	6	3.43	5	3	0.40	2.25	15	
12	4	2.88	50	3	0.40	2.25	15	
13	6	1.4	5	1.71	0.40	2.25	15	
14	2	2.96	5	2.33	0.40	2.25	15	
15	6	3	10	1.83	0.40	2.25	15	

take place, with a consequent slacking of the suspending hangers, that the proposed deformable section model allows to reproduce, differently from the classical 2-d-o-f model.

The relation between the forcing pulsation Ω_c or Ω_d and the pulsations ω_3 or ω_4 of the excited relative mode, is expressed through detuning parameters σ_3 , σ_4 defined by

$$\sigma_3 = \frac{\Omega - \omega_3}{\omega_3} (\Omega = \Omega_c, \Omega_d), \quad \sigma_4 = \frac{\Omega_d - \omega_4}{\omega_4} \quad (10)$$

The main results of the numerical investigation are reported in Fig. 5 to Fig. 13 and discussed in Sect. 5. The ranges of variation of the mechanical parameters and of the forcing characteristics adopted are representative of situations of long span suspended bridges, even if, in order to highlight the potentiality of the proposed sectional model, sometimes the forcing intensity has been assumed larger than generated by vortex shedding, as underlined in the Sect. 5. For example, with the assumed numerical values (cf. Table 1): the frequency $\omega_1=\alpha_1\omega_y$ of the vertical mode ranges between 0.20 rad/s and 2 rad/s, comparable to the corresponding values of typical bridges (e.g. 0.44 rad/s for the Akashi-Kaykio bridge and 1.4 rad/s for the Vincent Thomas bridge); the ratio α_2 between the torsional and the vertical global frequencies ranges between 1.4 and 3.4, corresponding to typical values (around 1.33 for the Messina Bridge, and 2.2 for the Akashi-Kaykio); the values of the ratio α_3 between the relative and global vertical modes, ranging between 4 and 160, include both the situations of relatively short bridges with a stiff deck (lower values) and the limit situations of decks with negligible stiffness in comparison with the stiffness of the suspensions system (cf. also Part I of the paper). On the other hand, the main aim of this paper was to stimulate a discussion on the actual possibility of this kind of phenomena.

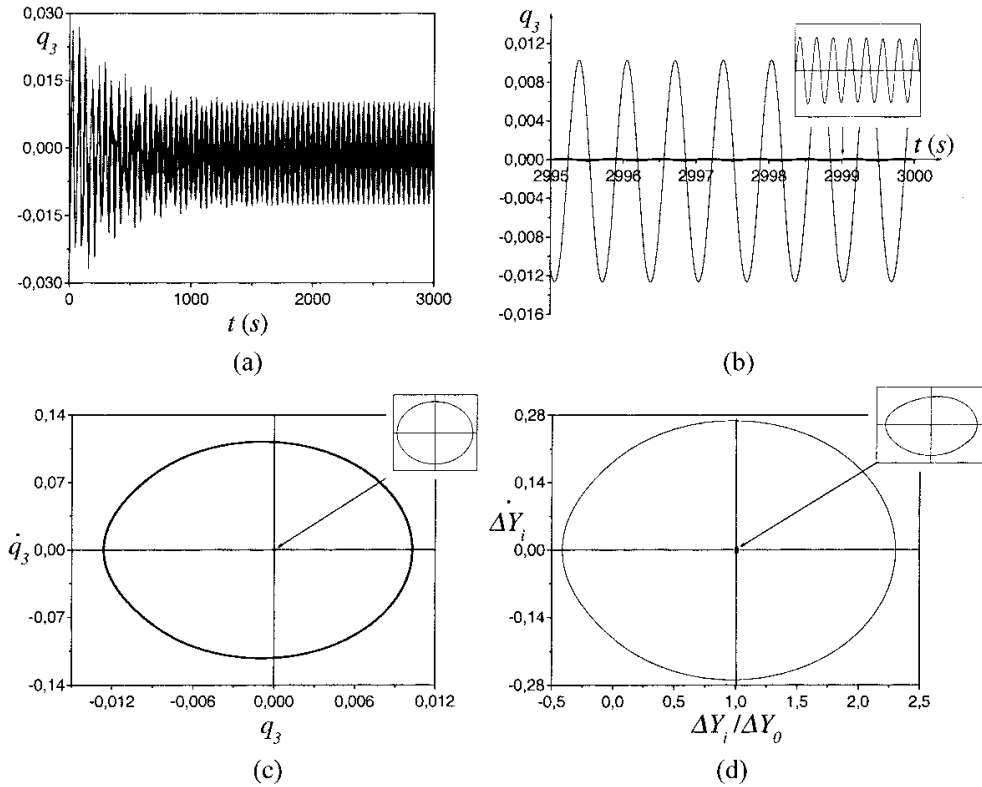


Fig. 5 Deck displacement q_3 and hangers elongation ΔY_i for case 4 of Table 1 ($\alpha_4=2.32$, no internal resonance). Transient (a) and stationary (b) time-history and stationary phase planes (c),(d) for load on the main cables of given pulsation, close to resonance with the relative vertical mode: $\Omega_c=0.95\omega_3$ ($\sigma_3=-0.05$), $f_c=0.0025$ (0.25% of the cable weight $m_c g$), $\Delta\varphi=\pi/4$, $\zeta_c=0.002$, $\zeta_y=0.003$, $\zeta_\theta=0.005$

5. Numerical investigation and discussion

5.1. Typical results

The time histories of the responses have been obtained by step-by-step numerical integration of the equations of motions, Eq. (3), with the discontinuity conditions of Eq. (8). In all cases, unless explicitly indicated, steady state response are reported (i.e., the values obtained when the amplitudes of velocities and displacements have stabilised). As examples, however, time-histories of the transient part of the response have also been included in Figs. 5(a) and 7(a).

Numerical investigations were performed on all cases in Table 1 for several different forcing on the main cables or on the deck. Because of space limitations, only a limited portion of the results obtained can be presented here; full details are reported in Diaferio (2002).

Fig. 5 shows the steady-state time-histories and phase-planes of vertical displacements of the deck centroid obtained for case 4 in Table 1, with no internal resonance between vertical and torsional relative modes, for a given frequency and intensity of the forcing action on the main cables. For the same case and the same forcing intensity, Fig. 6 reports the amplitude of the response as a function

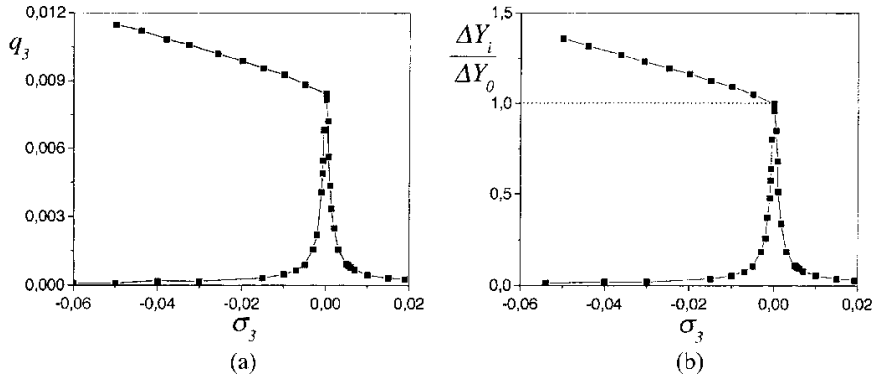


Fig. 6 Deck displacement and hangers elongation for case 4 of Table 1 ($\alpha_4=2.32$, no internal resonance). Frequency-response curves for load on the main cables, nearly resonant with the relative vertical mode: $\sigma_3=(\Omega_c-\omega_3)/\omega_3$, $f_c=0.0025$, $\Delta\varphi=\pi/4$, $\zeta_c=0.002$, $\zeta_y=0.003$, $\zeta_\theta=0.005$. (a) Vertical displacement of the deck, (b) Elongation of the hangers

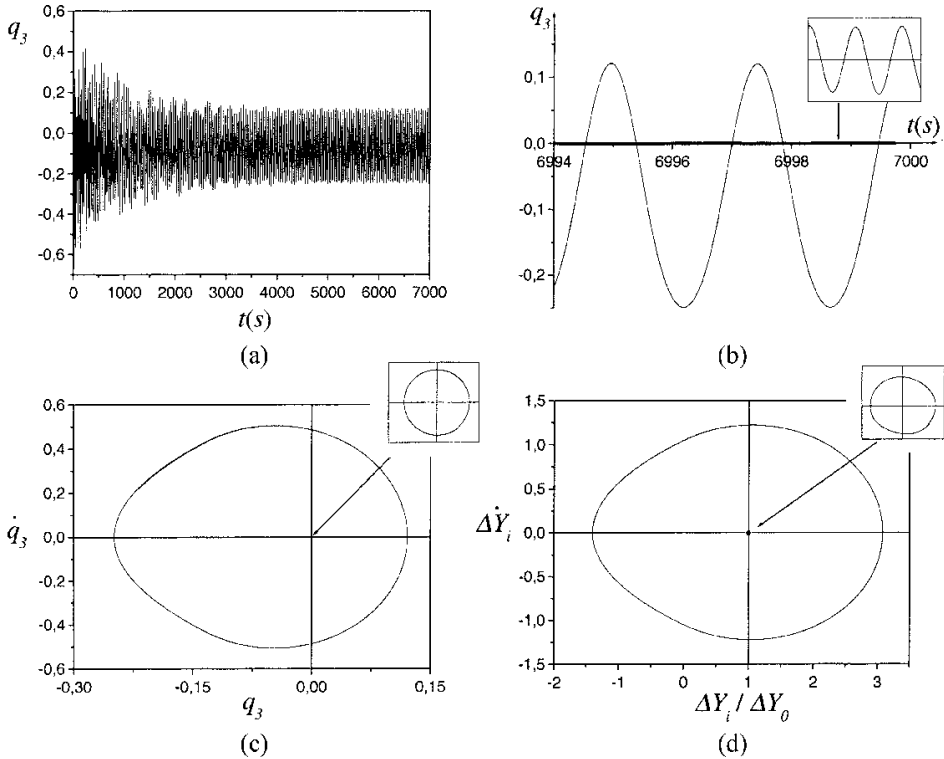


Fig. 7 Deck displacement q_3 and hangers elongation ΔY_i for case 1 of Table 1 ($\alpha_4=2.32$, no internal resonance). Transient (a) and stationary (b) time-histories and stationary phase planes (c),(d) for centric ($e_d=0$) load on the deck of given pulsation, close to resonance with the relative vertical mode: $\Omega_d=0.85\omega_3$ ($\sigma_3=-0.15$), $f_d=0.005$, $\zeta_c=0.002$, $\zeta_y=0.003$, $\zeta_\theta=0.005$

of the forcing frequency, at several values near to the frequency of the relative vertical motion.

Fig. 7 shows, in terms of time-histories and phase-planes, the response of the case 1 of Table 1 to

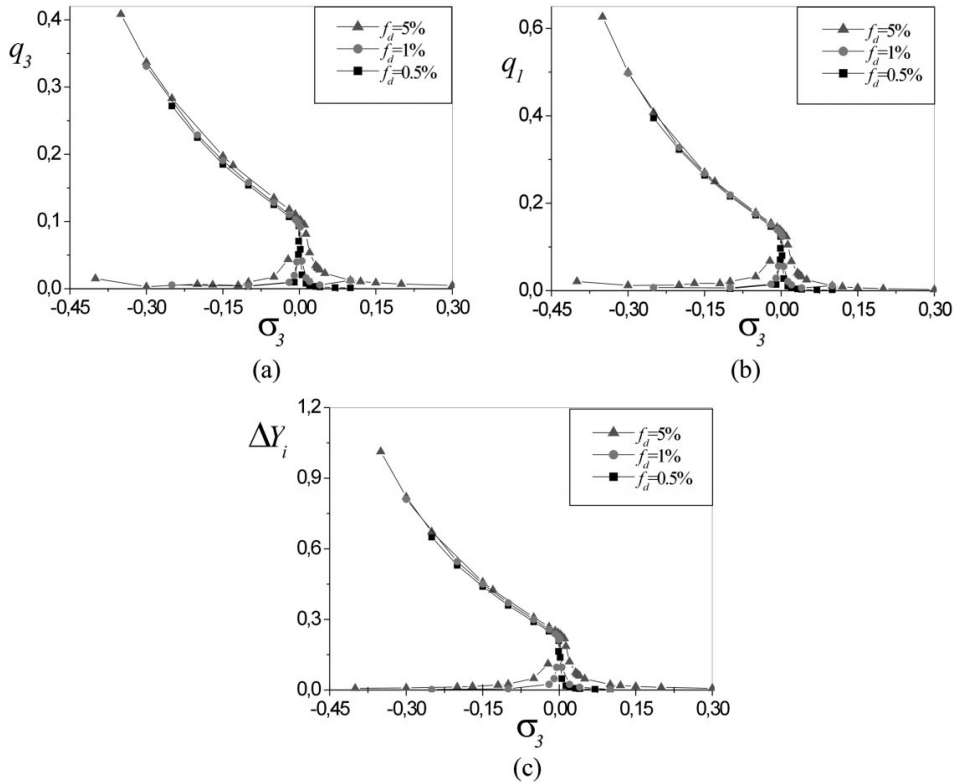


Fig. 8 Deck and cables displacements and hangers elongation for case 1 of Table 1 ($\alpha_4=2.32$, no internal resonance). Frequency-response curves for centric ($e_d=0$) load on the deck, close to resonance with the relative vertical mode: $\sigma_3=(\Omega_d-\omega_3)/\omega_3$, f_d varying between 0.005 and 0.05 (0.5 to 5% of the deck weight m_dg), $\zeta_c=0.002$, $\zeta_y=0.003$, $\zeta_\theta=0.005$; (a) vertical displacement of the deck, (b) vertical displacement of the main cables, (c) elongation of the hangers

an action of given frequency and intensity, assumed acting on the deck along the bridge axis (eccentricity $e_d=0$, cf. Eq. (5)); Fig. 8 reports, for different intensities of the force acting on the deck, the frequency-response curves around the natural frequency of the relative vertical mode. However, while the forcing intensities $f_c=0.5\%$ and 1% are compatible with vortex shedding under realistic wind speeds, the higher value $f_c=5\%$ must be considered only as a limit assumption.

In case of internal resonance between the vertical and torsional relative modes (case 2 of Table 1) the response to a centric force acting on the deck is illustrated in Fig. 9 through the phase-planes for a given forcing frequency, and in Fig. 10 through the frequency-response curves; the damping introduced in this case ($\zeta_y=\zeta_\theta=0.001$) is smaller than in the other ones, to highlight the effects of the internal resonance.

For the same geometrical and mechanical parameters of the internally resonant case 2 of Table 1, Fig. 11 shows the response to an eccentric force acting on the deck and near-resonant with the relative torsional mode.

For a given intensity of the load on the main cables, close to resonance with the vertical relative mode, Fig. 12 compares the responses for different values of the ratio α_1 (cf. Eq. (9)), that correspond to the cases 1, 3 and 4 (no internal resonance) in Table 1: note that α_1 is smaller when

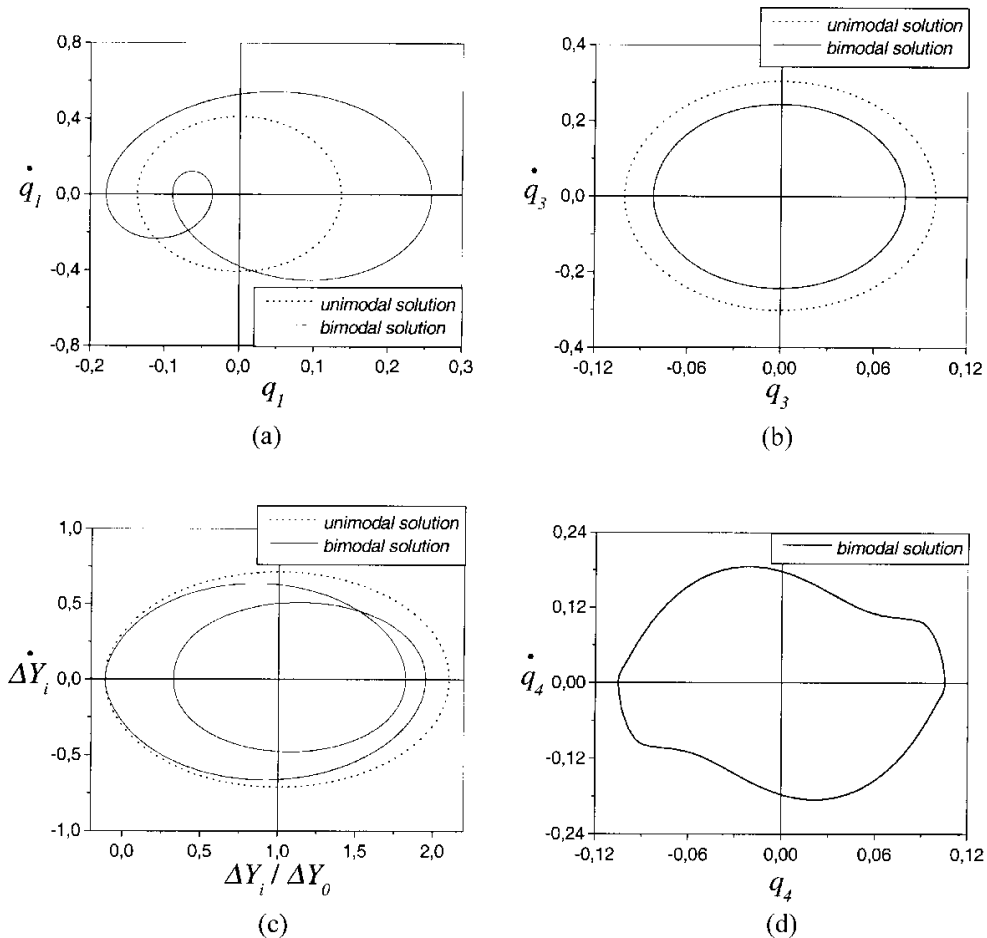


Fig. 9 Deck and cables displacements and hangers elongation for case 2 of Table 1 ($\alpha_4=2$, internal resonance). Phase-planes for centric ($e_f=0$) load on the deck with a given pulsation, close to resonance with the relative vertical mode: $\Omega_d=0.995\omega_3$ ($\sigma_3=-0.005$), $f_d=0.02$, $\zeta_c=0.002$, $\zeta_y=0.001$, $\zeta_\theta=0.001$ (a) vertical displacement of the main cables, (b) vertical displacement of the deck, (c) elongation of the hangers, (d) torsional rotation of the deck

the deck stiffness is larger with respect to the stiffness of the cables, i.e., when the span is shorter.

Similarly, Fig. 13 compares the frequency-response curves to the same type of excitation (force on the deck, near-resonant with the relative vertical mode) for different values of the parameter α_3 , that indicates the stiffness of the secondary suspension system (hangers) with respect to the stiffness of main cables and deck; they correspond to the cases 5 to 8 (no internal resonance) in Table 1.

In Figs. 12 and 13, to highlight the effects of the stiffness reduction due to the slacking of the hangers, values of the forcing intensity have been considered that, depending on the case, can be significantly larger than realistic.

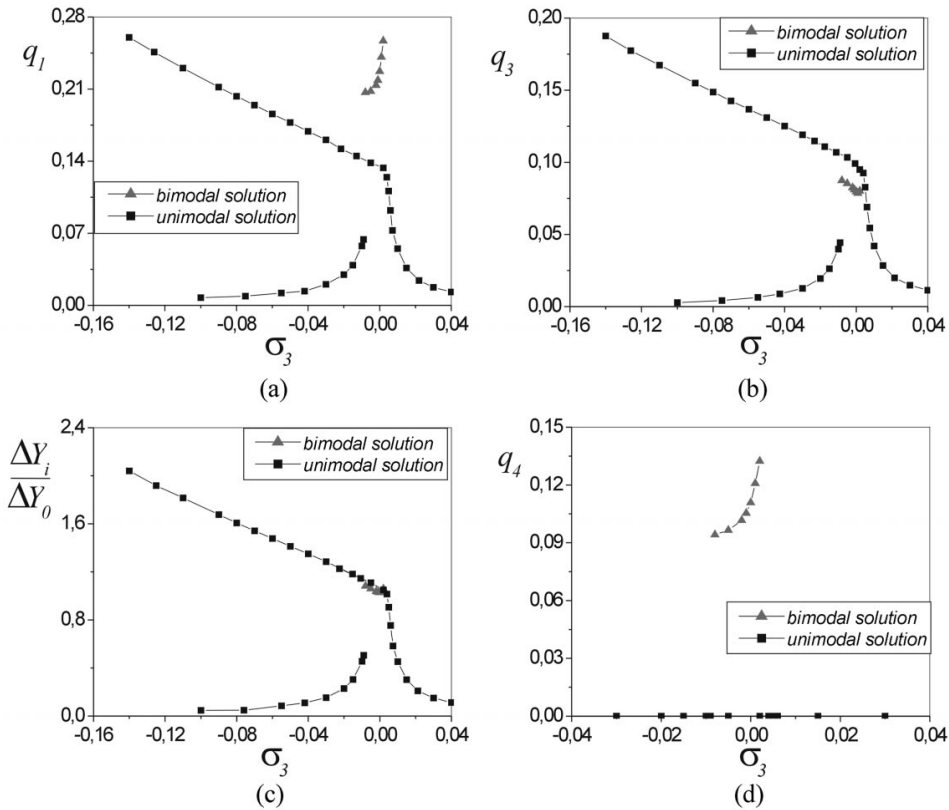


Fig. 10 Deck and cables displacements and hangers elongation for case 2 of Table 1 ($\alpha_4=2$, internal resonance). Frequency-response curves for centric ($e_d=0$) load on the deck, nearly resonant with the relative vertical mode: $\sigma_3=(\Omega_d-\omega_3)/\omega_3$, $f_d=0.02$, $\zeta_c=0.002$, $\zeta_y=0.001$, $\zeta_\theta=0.001$ (a) vertical displacement of the main cables, (b) vertical displacement of the deck, (c) elongation of the hangers, (d) torsional rotation of the deck

5.2. Discussion: effects of the properties of the action (frequency and intensity)

Consider, as a typical example, the structural system with $\alpha_1=20$, $\alpha_2=3$, $\alpha_3=5$ (case 4 in Table 1), subjected on the suspension cables to an action with pulsation close to the pulsation ω_3 of the relative vertical motion between deck and cables.

When the action amplitudes are comparatively small (in the example considered smaller than approximately 0.20% of the weight of a cable, $f_c < 0.0020$), the hangers turn out to be always taut, and the oscillations, always with small amplitude, are practically coincident with those given by the linear model and result asymptotically stable and symmetric with respect to the (static) equilibrium configuration.

For a forcing amplitude higher than this threshold value, instead, the model can show small or large amplitude oscillations, depending on initial conditions. In particular, Fig. 5 reports the responses of the model (both transient and stationary) caused by a forcing amplitude equal to 0.25% of the weight of the cables ($f_c=0.0025$) and pulsation $\Omega_c=0.95\omega_3$ ($\sigma_3=-0.05$), with phase-lag $\Delta\varphi=\pi/4$.

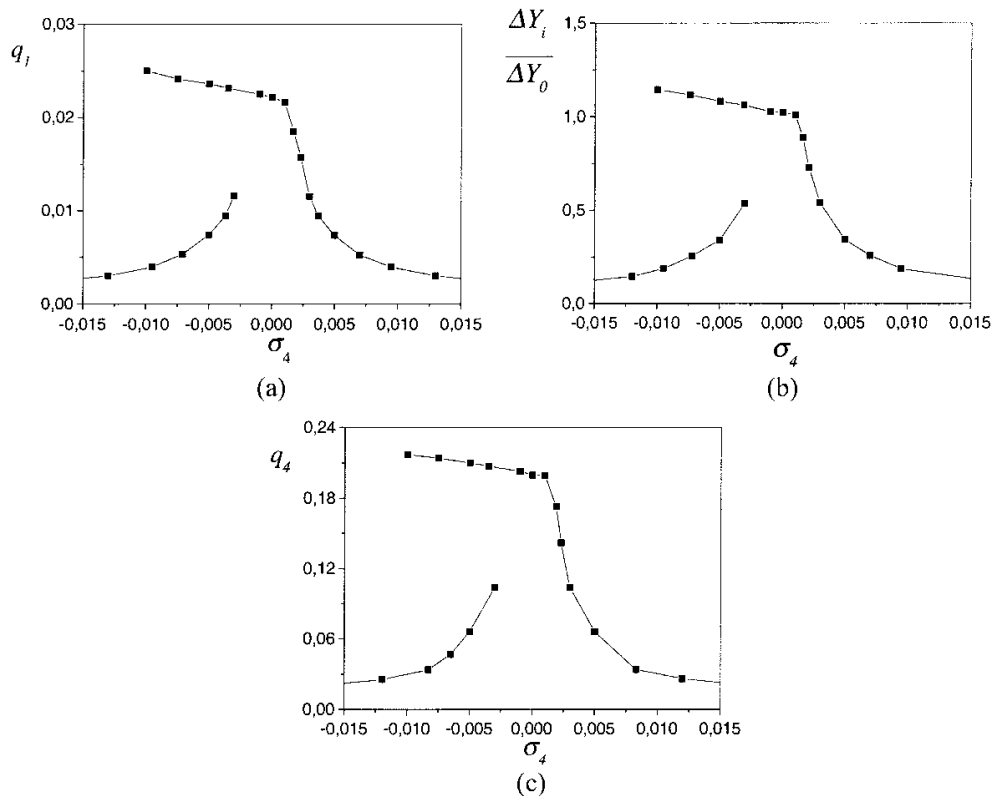


Fig. 11 Deck and cables displacements and hangers elongation for case 2 of Table 1 ($\alpha_4=2$, internal resonance). Frequency-response curves for eccentric load on the deck, nearly resonant with the relative torsional mode: $\sigma_4=(\Omega_d-\omega_4)/\omega_4$, $f_d=0.02$, $e_d=b/3$, $\zeta_c=0.002$, $\zeta_y=0.003$, $\zeta_\theta=0.002$ (a) vertical displacement of the main cables, (b) elongation of the hangers, (c) torsional rotation of the deck

When the pulsation is varied between $\Omega_c=0.94\omega_3$ and $\Omega_c=1.02\omega_3$ (Fig. 6) it can be noted that the steady-state amplitudes show a *softening* behaviour of the system; for a forcing frequency smaller than the frequency ω_3 of the relative vertical motion, two stable and periodic solutions coexist with the same frequency of the forcing action, but characterised by very different amplitudes of oscillation; as typical of this kind of systems, unstable solutions can also exist, but cannot be obtained by a step-by-step numerical integration; indeed they are not crucial for the objectives of this paper.

While small amplitude oscillations practically coincide with those that can be forecast through the 2-d-o-f linear model commonly used, large amplitude oscillations, corresponding to the slacking of hangers, can be even one or two orders of magnitude larger. These oscillations are non-symmetric with respect to the static equilibrium configuration (cf. Fig. 5), correspondingly to the non-symmetric constitutive behaviour of the secondary suspension (Fig. 2).

The behaviour so far described is analogous to the behaviour of 1-d-o-f systems with piece-wise linear restoring forces (Shaw and Holmes 1983, Natsiavas 1990), for which the plot in the phase-plane consists of two branches of ellipse with a common tangent in the intersection point.

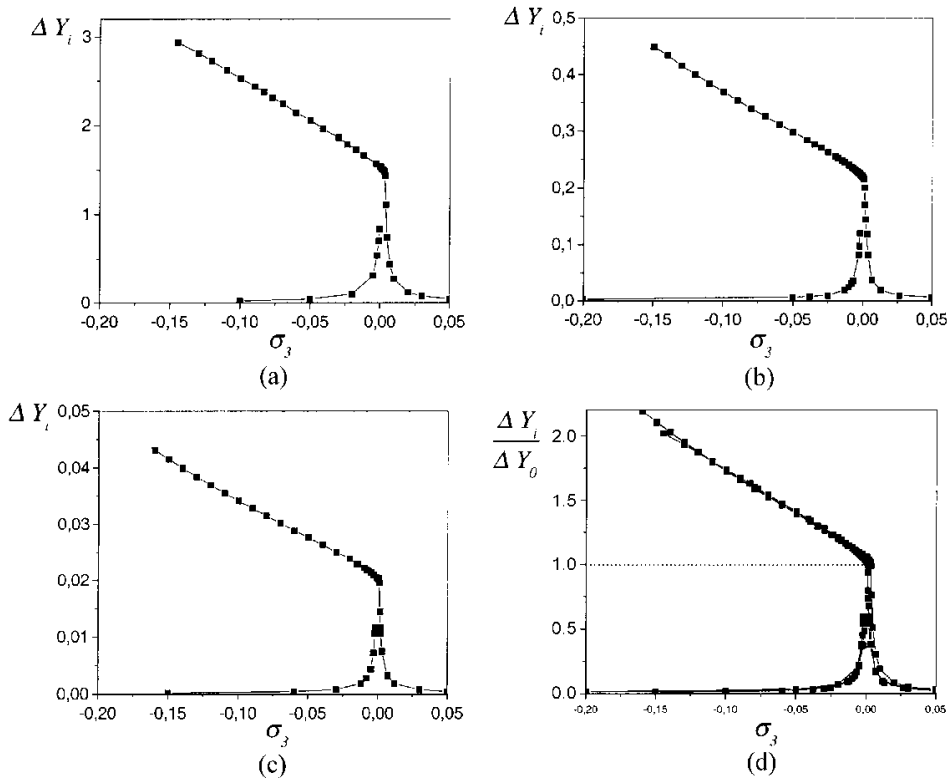


Fig. 12 Role of the stiffness of the suspension system (parameter α_1 in Eq. (9)) on the elongation of the hangers. (a) case 3 of Table 1, $\alpha_1=2$; (b) case 1, $\alpha_1=6$; (c) case 4, $\alpha_1=20$; for all cases $\alpha_4 \neq 2$ (no internal resonance), $\zeta_c=0.002$, $\zeta_y=0.003$, $\zeta_\theta=0.005$. Frequency-response curves for load on the main cables, nearly resonant with the relative vertical mode: $\sigma_3=(\Omega_c-\omega_3)/\omega_3$, $f_c=0.005$, $\Delta\varphi=\pi/4$. (d) elongation of the hangers normalised with respect to ΔY_0

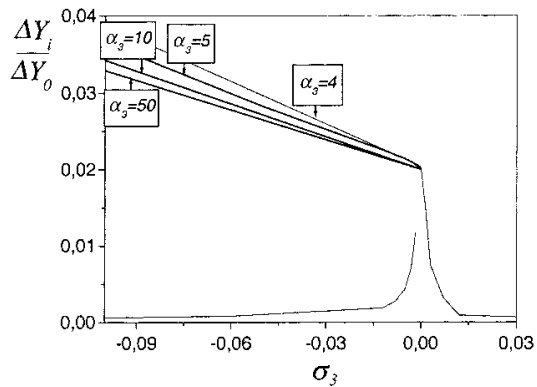


Fig. 13 Frequency-response curves of relative end displacement of the hangers for different α_3 (cases 5, 6, 7, 8 of Table 1) and forcing on the deck nearly-resonant with the relative vertical mode: $\sigma_3=(\Omega_d-\omega_3)/\omega_3$, $f_d=0.01$, $\alpha_4 \neq 2$ (no-internal resonance), $\zeta_c=0.002$, $\zeta_y=0.003$, $\zeta_\theta=0.005$

From the frequency-response curves reported in Fig. 6, a sharp “knee” in the slope of the backbone curve can be observed, due to a sharp modification of the stiffness characteristics of the system, differently from what can be found for systems with smooth nonlinearities, in which the slope of the backbone curve varies smoothly. As shown in the next Section, the change of slope in the knee of the backbone curve depends on the ratio between the stiffness of the secondary suspension system (hangers) and the stiffness of the deck, and therefore on the parameter α_3 .

In the same examples presented in Figs. 5-6, it has been noted that also for large amplitude motions the torsional oscillations due to the phase-lag between the actions on the main cables are of the same order of magnitude of those given by the linear model, and this independently of the value of the phase-lag (as confirmed by results presented in Diaferio 2002); this is due to the absence of internal resonances between the relative vertical component of the motion, directly excited, and the relative torsional component, with a higher frequency.

The behaviour of the system is similar with actions applied on the deck (Fig. 7, Fig. 8); for forcing frequencies smaller than the natural one ω_3 , also in this case two stable solutions with the same frequency and different amplitude may coexist with unstable solutions, that cannot be found through numerical integration.

Also for a forcing action on the deck, the plot in the phase-plane (Fig. 7(c),(d)) is analogous to that described by Shaw and Holmes (1983) for a 1-d-o-f model with piece-wise restoring force. And also this time, without internal resonance, the absence of torsional components of the action ($e_d=0$) implies, even for large amplitude oscillations and for large f_d , the absence of torsional rotations.

The behaviour is completely different in case of internal resonance between the relative vertical and torsional modes ($\alpha_4=2$). In this case, in fact, even if the action on the deck is not eccentric, a relative torsional motion can start for appropriate initial conditions, with amplitude comparable to that of the vertical motion, and this kind of behaviour cannot be forecast by means of the classical 2-d-o-f sectional model.

This condition is shown by the examples whose main results are presented in Figs. 9 and 10, for a centric action on the deck with angular frequency close to ω_3 . It is possible to individuate two classes of large amplitude oscillations, both stable for the values of parameters under consideration (apart from unstable solutions, not found numerically). The first solution (defined *unimodal*, see Fig. 9 and 10) has the same period than the action, and is analogous to the solutions of the cases already discussed, i.e., is characterised by oscillations of the system in the vertical plane only, with in-phase motion of the main cables and no torsional rotations. In the second solution (called *bimodal*, and found only in a small range of frequencies) the vertical component of the deck motion has the same period of the forcing action, but torsional oscillations are also present, with period multiple of the forcing period (subharmonic response): these torsional rotations are due to the energy transfer from the directly excited vertical mode to the internally resonant torsional one.

Finally, Fig.11 shows the effect of an eccentricity e_d of the action on the deck, again in case of internal resonance between the relative vertical and torsional modes ($\alpha_4=2$), but this time synchronised with the frequency ω_4 of the relative torsional mode between main cables and deck. The frequency-response curves of the torsional rotation and of the length variation of the hangers (Fig. 11(b),(c)) underline the coexistence of small and large amplitude solutions, while, notwithstanding the internal resonance, the vertical oscillations of the deck turn out small, of the same order of magnitude of those that could be obtained with the classical 2-d-o-f sectional model, because this time the excited mode is the higher frequency one.

In all cases considered, it can be observed that the deck oscillate around an average configuration

different from the initial one, as a consequence of the non-symmetric behaviour of the hangers: this is the more evident as the larger are the oscillations.

5.3. Discussion: effects of mechanical parameters

In this Section the role of the mechanical parameters of the system is examined, again in the case of actions on the main cables nearly resonant with the angular frequency ω_3 of the relative motion between main cables and deck. Fig. 12 shows the frequency-response curves of the length variation of the hangers for three different values of the parameter α_1 ($\alpha_1=2$, $\alpha_1=6$ and $\alpha_1=20$), while other parameters are kept constant.

It can be observed that the different value attained by ΔY_i in the knee of the response curve (value that corresponds to $\Delta Y_i \cong \Delta Y_0$) can be explained considering that the value of α_1 is the larger the stiffer is the main suspension system; on the other hand, for increasing α_1 the parameter α_3 can be kept constant, as assumed, only if the hangers stiffness K_{h0} increases in the same ratio, with a consequent reduction of the initial elongation ΔY_0 under dead loads.

And in fact, if the relative displacement between the two ends of the hangers is normalised with respect to this value ΔY_0 , the frequency-response curves for different values of α_1 are almost coincident (Fig. 12(d)).

The role of the hanger stiffness, represented by the parameter α_3 , is shown in Fig. 13.

It can be observed that for an increasing stiffness of the secondary suspension system (hangers) and therefore of the parameter α_3 , the numerical evaluation of the steady-state solution becomes more and more difficult. According to the objectives of this paper, mainly devoted to describe in a general way the conditions under which large amplitude oscillations are possible and to characterise them, it has not been investigated if the numerical difficulties found for large values of α_3 (namely $\alpha_3=160$, case 9 of Table 1) are due to the algorithm used or are, instead, related to some intrinsic characteristics of the response (e.g., because it is non-periodic, or even chaotic).

On the other hand, the difficulties that have been found are justified considering that a system with $\alpha_3 > 50$ is analogous, in all respects, to the limit case in which the suspending hangers are modelled through unilateral constraints not deformable in traction, with consequent impulsive phenomena for each crossing of the discontinuity described by Eq. (8).

In similar cases, the great dependence of the response on the accuracy of numerical calculations (and on the initial conditions, of course) has already been noted by other Authors (e.g., Natsiavas 1990).

In the case of an action on the deck with frequency close to ω_3 , and without internal resonance, the role has been investigated of the parameter α_2 that characterises the global torsional stiffness of the system, whose values have been varied between 1.4 and 3.23; the numerical results, reported in detail in Diaferio (2002), show that α_2 does not influence the structural response when the forcing is not eccentric.

6. Conclusions

A 4-d-o-f sectional model, able to describe the wind-induced response of long-span bridges taking into account the longitudinal deformability of the unilateral hangers, has been proposed and analyzed. In Part I (Sepe and Augusti 2001) the elastic response and its limits have been investigated, while this Part II investigates numerically the non-linear behaviour under harmonic

actions on the cables and on the deck, like those that could be e.g., generated by vortex shedding.

The oscillations started by such actions on the main cables or on the deck have been sought by numerical integration of the ordinary differential equations that describe the motion (Eq. (3)); outside the range of small oscillations, in fact, these equations become nonlinear due to the unilateral behaviour of hangers.

The results reported here underline that as a consequence of this characteristic behaviour of the suspending hangers, it is possible to observe oscillations with amplitude one or two orders of magnitude larger than those evaluated through the classical 2-d-o-f sectional model (hangers without elongation), with a dynamic behaviour particularly interesting and complicated when internal or external resonance conditions occur.

To simplify the approach, the numerical investigations performed so far have assumed a harmonic action, in order to catch at least the main aspects of the response under loads induced by vortex shedding (Simiu and Scanlan 1996). Possible developments of the research should include a more accurate modelling of this kind of actions (e.g., D'Asdia, *et al.* 1998).

The deformable section model could also allow to evaluate the wind induced oscillations (buffeting) in the sub-critical range of wind speed, i.e., far from self-excited or resonant oscillations. Also of interest are the relative oscillations due to the different nature and intensity of the wind actions on the main cables and the deck, which for very long span bridges are significantly distant from each other.

A possible further improvement of the model might be to attribute (by numerical techniques) to the stiffness reduction coefficient δ_1 values in the whole range between 0 and 1, depending on how many hangers are slack. Along a similar line, the model could also be extended to describe the local motion of a part of the bridge, taking into account, for example, higher vibration modes of the cables, with frequencies in between those of the pseudo-modal shapes here considered, depending on the wave length.

To describe local oscillations and/or travelling waves a convenient alternative to the sectional model may be the technique of "equivalent" nonlinearisation proposed in the PhD thesis of one of the writers (Diaferio 2000, Diaferio and Sepe 2001); it consists in the substitution of each row of unilateral hangers with a suspension system characterised by a regular constitutive law, made equivalent through an energy criterion to the real one. This allows to obtain continuous models with smooth nonlinearities (polynomial, in Diaferio 2000, Diaferio and Sepe 2001), for which, under periodic action, it is possible to obtain closed form solutions through perturbative techniques.

All such studies tend to show that suspension bridges much longer than existing ones might experience unusual (and unexpected) phenomena, that have sometimes been described by several Authors (McKenna, Walter 1987): these results should warn designers not to limit *a priori* their considerations to phenomena already observed and studied for existing bridges.

To this respect, the paper aims at stimulating discussion on the possibility of the phenomena described, whose actual significance can be assessed only through *ad hoc* calculations and specific experimental research.

Acknowledgements

This paper has been prepared within the "Research Project of National Interest" (PRIN) on Wind Engineering WINDERFUL, partially supported by the Italian Ministry for Instruction, University and Research. Some of the results reported here have been included in the paper presented by the

writers to the seventh Italian Conference on Wind Engineering (Augusti, *et al.* 2002).

Notation

ΔY_i	amplitude of the relative displacement between i -th main cable and deck
ΔY_0	elastic elongation of the hangers in the reference configuration
t	time
$\psi(x)$	longitudinal shape
$Y(t)$	generalised displacement of the deck
$\Theta(t)$	generalised rotation of the deck
$Z_1(t), Z_2(t)$	generalised displacement of the two main cables
m_c	generalised mass of each cable
m_y	generalised mass of the deck
I	generalised torsional inertia of the deck
ζ_c	damping coefficient of the main cables
ζ_y	damping coefficient of the vertical motion of the deck
ζ_θ	damping coefficient of the torsional motion of the deck
b	half-width of the deck
ω_c	natural pulsation of cables
ω_y	vertical natural pulsation of the deck, considered as isolated
ω_θ	torsional natural pulsation of the deck, considered as isolated
K_c	vertical generalised stiffness of each cable
K_y	vertical generalised stiffness of the deck
K_θ	torsional generalised stiffness of the deck
K_{h0}	generalised stiffness of a row of hangers
$\delta_i (i=1,2)$	stiffness-reduction coefficient that takes into account the possible “slacking” of the hangers
F_{c1}, F_{c2}	vertical forces acting on the main cables
F_y	vertical force acting on the deck
M_θ	moment acting on the deck
q_1, q_2	non-dimensional generalised displacement of the main cables
q_3	non-dimensional generalised vertical displacement of the deck
q_4	non-dimensional generalised torsional rotation of the deck
d_0	non-dimensional elastic elongation of the hangers in the reference configuration
g	gravitational acceleration
f_1, f_2	non-dimensional vertical forces acting on the main cables
f_3	non-dimensional vertical force acting on the deck
f_4	non-dimensional moment acting on the deck
$\beta_1 = m_c/m_y$	cable to deck mass-ratio
$\beta_2 = m_c b^2/I$	cables to deck rotational-inertia-ratio
$w_h^2 = K_{h0}/m_c$	
f_c	amplitude of the actions on the main cables
Ω_c	pulsation of the force on the cables
Ω_d	pulsation of the force on the deck
$\Delta\varphi$	phase lag between the forces acting on the cables
f_d	force amplitude on the deck
e_d	eccentricity between the direction of the force and the centre of the deck
ω_1	pulsation of the global vertical mode
ω_2	pulsation of the global torsional mode
ω_3	pulsation of the relative vertical mode
ω_4	pulsation of the relative torsional mode
α_1	ratio between the pulsation ω_1 of the first <i>global</i> bending mode of the system and the pulsation ω_y of the analogous mode of the deck alone

- α_2 ratio between the pulsation ω_2 of the *global* linear torsional oscillation and the corresponding bending pulsation ω_1
- α_3 ratio between the pulsation ω_3 of the *relative* vertical deck-cables motion and the system *global* bending pulsation ω_1
- α_4 ratio between the pulsation ω_4 of the *relative* torsional deck-cables motion and the system *relative* vertical deck-cables motion ω_3
- $\sigma_3 = (\Omega - \omega_3) / \omega_3$ ($\Omega = \Omega_c, \Omega_d$) detuning parameter
- $\sigma_4 = (\Omega_d - \omega_4) / \omega_4$ detuning parameter

References

- Augusti, G., Diaferio, M. and Sepe, V. (2002), "Unilateral behaviour of the suspending hangers in the wind induced response of large span bridges", *7th Italian Conference on Wind Engineering IN-VENTO-2002*, Milano (Italy).
- Augusti, G., Sepe, V. and Della Vedova, M. (1997), "A nonlinear model for the analysis of wind-induced oscillations of suspension bridges", *Proc. 2nd Euro-African Conference on Wind Engineering*, Genoa, 22-26 June, **2**, 1617-1624.
- Augusti, G. and Sepe, V. (1999), "A deformable section model of large suspension bridges: the limit condition for linear response", *Proceedings of the Fourth European Conference on Structural Dynamics EURO-DYN '99*, Prague, June 1999, **2**, 771-776.
- D'Asdia, P., Noè, S. and Viskovic, A. (1998), "Distacco di vortici da un corpo elastico cilindrico a sezione circolare: un nuovo modello numerico autolimitante ed autoregolato", *5th Italian Conference on Wind Engineering IN-VENTO-98*, Perugia (Italy), 135-146 (*In Italian*).
- Diaferio, M. (2000), "Modelli non lineari di strutture elastiche sospese", Ph.D. Thesis, University of Florence (Italy) (*In Italian*).
- Diaferio, M. (2002), Report on a numerical investigation for the Department of Structural and Geotechnical Engineering, Università di Roma "La Sapienza" (*In Italian*).
- Diaferio, M. and Sepe, V. (2001), "Modelli continui non lineari per ponti sospesi soggetti ad azioni eoliche", *15th Italian Conference on Theoretical and Applied Mechanics AIMETA 2001*, Taormina (Italy) (*In Italian, Proceedings on CD-ROM*).
- McKenna, P.J. and Walter, W. (1987), "Nonlinear oscillation in a suspension bridge", *Archive of Rational Mechanics and Analysis*, **98**, 167-177.
- Natsiavas, S. (1990), "On the dynamics of oscillators with bilinear damping and stiffness", *Int. J. Nonlinear Mech.*, **25**(5), 535-554.
- Sepe, V. and Augusti, G. (2001), "A "deformable section" model for the dynamics of suspension bridges. Part I: Model and linear response", *Wind and Structures*, **4**(1), 1-18.
- Simiu, E. and Scanlan, R.H. (1996), *Wind Effects on Structures*, J. Wiley & Sons, 3rd Edition.
- Shaw, S.W. and Holmes, P.J. (1983), "A periodically forced piecewise linear oscillator", *J. Sound Vib.*, **90**(1), 129-155.